Imaging Agents

International Edition: DOI: 10.1002/anie.201813397
German Edition: DOI: 10.1002/ange.201813397

A Noncovalent Fluorescence Turn-on Strategy for Hypoxia Imaging

*Wen-Chao Geng, Shaorui Jia, Zhe Zheng, Zhihao Li, Dan Ding, and Dong-Sheng Guo**

Dedicated to Professor Yu Liu on the occasion of his 65th birthday

Abstract: *Hypoxia plays crucial roles in many diseases and is a central target for them. Present hypoxia imaging is restricted to the covalent approach, which needs tedious synthesis. In this work, a new supramolecular host–guest approach, based on the complexation of a hypoxia-responsive macrocycle with a commercial dye, is proposed. To exemplify the strategy, a carboxyl-modified azocalix[4]arene (CAC4A) was designed that binds to rhodamine 123 (Rho123) and quenches its fluorescence. The azo groups of CAC4A were selectively reduced under hypoxia, leading to the release of Rho123 and recovery of its fluorescence. The noncovalent strategy was validated through hypoxia imaging in living cells treated with the CAC4A–Rho123 reporter pair.*

Hypoxia is a common feature in most of solid tumors that is ascribed to the imbalance between the increased oxygen consumption caused by rapid proliferation and an inadequate oxygen supply resulting from an altered tumor vasculature.[1] Hypoxia is correlated with increased metastasis[2] and increased resistance to radiotherapy, chemotherapy,[3] and photodynamic therapy.[4] It is also an indicator for tumor aggression[5] and an indicator of poor prognoses and therapeutic outcomes.[2] Accurate hypoxia detection and imaging could be helpful in terms of identifying hypoxic-tumor-bearing patients and formulating suitable clinical treatment plans.[6]

The low oxygen levels result in the imbalance of cellular redox states, causing an enhanced reductive stress.[7] The reduction potential and the activity of various bioreductive enzymes in hypoxic tumors and that in normoxic tissues are significantly different.[7,8] Taking advantage of the higher reductive stress, a variety of hypoxia-selective probes and drugs have been developed.[9] Most effort associated with hypoxia imaging and therapy has focused on the nitro group, which can be reduced to amine by nitroreductase.[10] Alternatively, another kind of reducible chemical group, the azo bond, was found to break in a reductive microenvironment and be reduced to aniline derivatives, with the actual chemical response being a function of oxygen partial pressure.[11] In the case of the azo group, little fluorescence is typically seen since the excited energy state is rapidly dissipated due to conformational changes around the azo bond.[12] This deactivation pathway is eliminated after reduction of the N=N double bond, thus leading to an increase in the fluorescence emission intensity.[13]

To the best of our knowledge, all reported efforts to implement hypoxia imaging through use of azo reduction have been based on a covalent strategy that involves linking an azo group to a dye (Scheme 1 a). However, direct covalent attachment approaches, although effective in terms of creating hypoxia-responsive systems, sometimes suffer from some disadvantages, including complicated molecular design, time-consuming and expensive synthesis, activity changes due to the covalent linker, and potential toxicity enhancement because of introducing an exogenous moiety on dyes.[11] Moreover, each azo conjugate was only implemented for imaging or treating hypoxia by the linked agents.[11a,12] Supramolecules represent an alternative approach to produce stimuli-responsive biomedical systems that are more easily operated and universal.[14] With this regard, we are working to develop a noncovalent strategy based on the host–guest interaction between azocalixarene and dye (Scheme 1 b). In this strategy, a dye is pre-included into the cavity of an

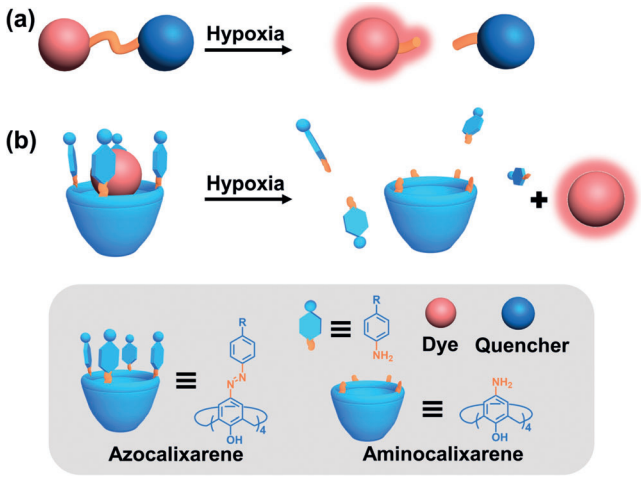

Scheme 1. Schematic illustration of the design principles of the conventional covalent (a) and the proposed noncovalent (b) strategies for creating hypoxia-responsive systems.

[*] W.-C. Geng, Z. Zheng, Z. Li, Prof. D.-S. Guo
College of Chemistry, Key Laboratory of Functional Polymer Materials (Ministry of Education), State Key Laboratory of Elemento-Organic Chemistry, Nankai University
Tianjin 300071 (China)
E-mail: dshguo@nankai.edu.cn
S. Jia, Prof. D. Ding
Key Laboratory of Bioactive Materials, Ministry of Education, College of Life Sciences, Nankai University
Tianjin 300071 (China)
Supporting information and the ORCID identification number(s) for the author(s) of this article can be found under: https://doi.org/10.1002/anie.201813397.

azocalixarene. This supramolecular complexation leads to a quenching of the fluorescence intensity. Upon encountering a hypoxic environment, the azo groups of the azocalixarene get reduced. This leads to the release of the dye and the recovery of the fluorescence intensity.

To achieve the imaging of hypoxia via such a noncovalent way, a tailored host–guest reporter pair is needed. The host is expected to 1) bind strongly towards commercial imaging dyes to avoid undesired off-target leaking,[14b] 2) "super"-quench the fluorescence to minimize the imaging background,[15] 3) most importantly, be hypoxia-responsive to release the entrapped dye to allow fluorescence recovery. Accordingly, we designed the artificial receptor 5,11,17,23-tetrakis[(*p*-carboxyphenyl)azo]-25,26,27,28-tetra-hydroxy calix[4]arene (CAC4A) (Figure 1a). Calixarenes were selected as the macrocyclic scaffold, which have been

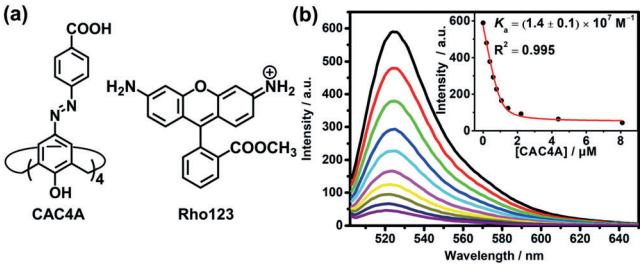

Figure 1. a) Molecular structures of CAC4A and Rho123. b) Direct fluorescence titration of Rho123 (1.0 μM) with CAC4A (up to 8.1 μM) in PBS buffer (pH 7.4) at 37 °C and the associated titration curve (inset) at $\lambda_{em} = 525$ nm and fit according to a 1:1 binding stoichiometry, $\lambda_{ex} = 500$ nm.

described as having "(almost) unlimited possibilities" due to their easy derivatization.[16] By directly reacting calix[4]arene with *p*-carboxybenzenediazonium chloride at 5 °C for two hours, CAC4A was obtained with quantitative yield (for more details, see the Supporting Information).[17] Rhodamine 123 (Rho123) is a commercial fluorescent dye and has been widely used in bioimaging owing to its high brightness and photostability.[18] Rho123 was employed as the reporter dye due to the strong complexation with CAC4A and the corresponding drastic fluorescence quenching (Figure 1b). A Job's plot determined the 1:1 binding stoichiometry between CAC4A and Rho123 (Supporting Information, Figure S2). The association constant (K_a) was determined as $(1.4 \pm 0.1) \times 10^7\,\text{M}^{-1}$ by fitting the data of the fluorescence titration (Figure 1b, inset). Such a strong binding is desirable to reduce unwanted cargo–carrier dissociation of reporter pair, especially for use in complex biological conditions. In contrast to covalent methods, the present noncovalent strategy faces the challenge of the competitive complexation of biologically coexisting species with CAC4A, which would lead to release of Rho123 and give rise to imaging noise. The changes in the fluorescence intensity of CAC4A–Rho123 resulting from biologically important species (adenosine triphosphate, amino acids, metal ions, glucose, urea, creatinine, and bovine serum albumin) were tested (Supporting Information, Figure S3). No significant increases in the fluorescence intensity of CAC4A–Rho123 were observed in the presence of these biological species. As a result, the extremely strong binding between CAC4A and Rho123 resists the interference from biologically coexisting species.

The complexation between Rho123 and CAC4A was further studied by ^{1}H NMR spectroscopy. In the presence of CAC4A, Rho123 protons showed upfield shifts (Supporting Information, Figure S4) caused by the ring current effect of the aromatic nuclei of calixarenes.[19] The shifts of benzene protons (H4 to H7) are larger than xanthene protons (H1 to H3), indicating that the benzene part of Rho123 is encapsulated more deeply inside the cavity of CAC4A. The calixarene protons also underwent upfield shifts affected by Rho123. The assumed binding geometry was further validated by the 2D NOESY spectrum (Supporting Information, Figure S5). We observed the intermolecular correlations between benzene protons of Rho123 and phenolic protons of CAC4A, and also correlations between xanthene protons of Rho123 and substituted benzoic acid protons of CAC4A. Geometry optimization[20] reveals that the CAC4A–Rho123 complex assumes a size-matching model. The benzene part of Rho123 locates at the centre of the cavity and xanthene part is at upper rim (Figure 2a), which is in good agreement with the NMR results. The optimized structure of CAC4A–Rho123 displays three evident intermolecular hydrogen bonds: two N–H···O (1.71 and 1.73 Å) between carboxyl groups of CAC4A and amino groups of Rho123 and one C–H···O (2.24 Å) between an aromatic hydrogen of CAC4A and the carbonyl oxygen of Rho123. To obtain further insights into the host–guest interactions, the molecular electrostatic poten-

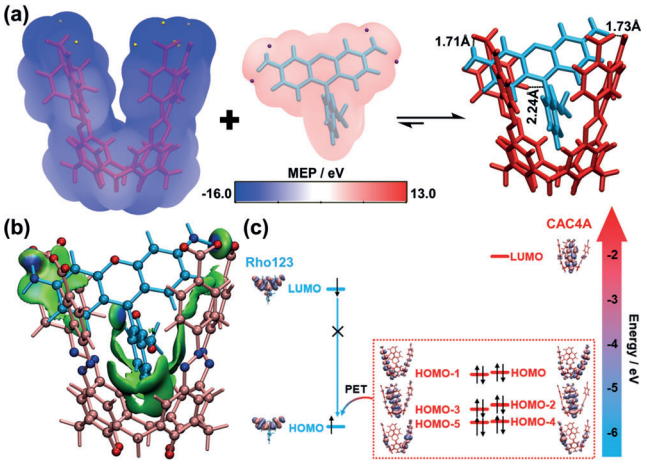

Figure 2. a) Optimized binding geometry of the CAC4A–Rho123 complex (right) at the B3LYP-D3/6-31G(d)/SMD(water) level of theory and MEP-mapped molecular vdW surface of CAC4A (left) and Rho123 (middle). The highest four MEP maxima of Rho123 and the lowest seven minima of CAC4A are shown by purple and yellow dots, respectively. Evident hydrogen bonds are shown by dashed lines. b) $\delta g^{inter} = 0.007$ a.u. isosurfaces colored according to a blue-green-red scheme over the range $-0.05 < \text{sign}(\lambda_2)\rho < 0.05$ a.u. for CAC4A–Rho123 complex (the meaning of δg^{inter} and $\text{sign}(\lambda_2)\rho$ can be found in ref. [22]). Blue indicates a strong attraction, and red indicates a strong repulsion. c) Frontier orbital energy diagrams and the electron-transfer path from CAC4A to Rho123.

tial[21] (MEP) mapped on the van der Waal (vdW) surface of CAC4A and Rho123 was computed (Figure 2a). CAC4A is electron-rich, especially at the upper rim, and Rho123 is electron-deficient, especially at the amino groups. The optimized geometry is favorable because molecules always tend to interact with each other in a MEP-complementary manner. The independent gradient model analysis[22] (Figure 2b) not only validates the existence of three hydrogen bonds (blue area in isosurfaces) but also reveals π-stacking interactions (green area in isosurfaces) between CAC4A and Rho123. Collectively, the high binding affinity between CAC4A and Rho123 originates from the synergistic effect among multiple, noncovalent interactions (electrostatic, hydrogen bonding, and π-stacking).

The fluorescence quenching of Rho123 upon binding with CAC4A (I_{free}/I_{bound}) is calculated as 14, which is appropriate for the subsequent application of hypoxia imaging. The mechanism of the binding-induced fluorescence quenching is vital for understanding the supramolecular hypoxia imaging strategy. Widely studied covalent hypoxia imaging probes rely on quenching mechanisms of Förster resonance energy transfer (FRET)[11a] or ultrafast conformational change of the azo part in the excited state.[12] The absorption of CAC4A shows no appreciable overlap with the emission of Rho123 (Supporting Information, Figure S6), ruling out the FRET quenching. Moreover, the fluorescence quenching of Rho123 resulting from the conformational change of the azo groups of CAC4A is unlikely because CAC4A and Rho123 form a noncovalent complex, not a covalent conjugate.[12,23] Alternatively, CAC4A could quench the fluorescence of Rho123 via the photoinduced electron transfer (PET) mechanism.[24] Calixarenes are well-demonstrated fluorescence quenchers via the PET mechanism.[25] The PET process between CAC4A and Rho123 was rationalized by simple molecular orbital theory,[26] which is a prevalent tool used to discuss the fluorescence on-off problem.[27] The HOMO energy of Rho123 is lower than energies of six occupied orbitals (HOMO to HOMO-5) of CAC4A (Figure 2c and Supporting Information, Table S1). This results in the occurrence of reductive-PET, in which an electron on the host transfers to the guest and fills its singly occupied HOMO. 4-((4-Hydroxyphenyl)diazenyl)benzoic acid (CA-phenol; Supporting Information, Scheme S1), the building subunit of CAC4A, was employed to explore the superiority of CAC4A. Although the higher HOMO energy of CA-phenol than that of Rho123 (Supporting Information, Table S1) permits the reductive-PET, only very slight quenching of fluorescence was observed upon adding CA-phenol to Rho123 solution (Supporting Information, Figure S7). Furthermore, the absence of quenching of Rho123 by 4-carboxyazobenzene (Supporting Information, Scheme S1; whose HOMO energy is lower than that of Rho123, as given in Table S1 in the Supporting Information) further validates the supposed PET mechanism (Supporting Information, Figure S7). The above phenomena indicate the irreplaceable role of calixarene in reaching two prerequisites of our strategy: 1) the preorganized skeleton ensures the strong complexation with Rho123; 2) the lower-rim phenolic hydroxyls enable the fluorescence quenching.

UV/Vis spectroscopy was employed to examine the hypoxia response of CAC4A. CAC4A displays a broad absorption peak longer than 400 nm (Supporting Information, Figure S8), attributed to n-π* transitions of the azo groups according to the natural transition orbital analysis (Supporting Information, Table S2). Upon addition of excess sodium dithionite (SDT), a chemical mimic of azoreductase,[23,28] a loss of the characteristic yellow color of CAC4A was detected within 10 min (Photos in Figure 3a). The

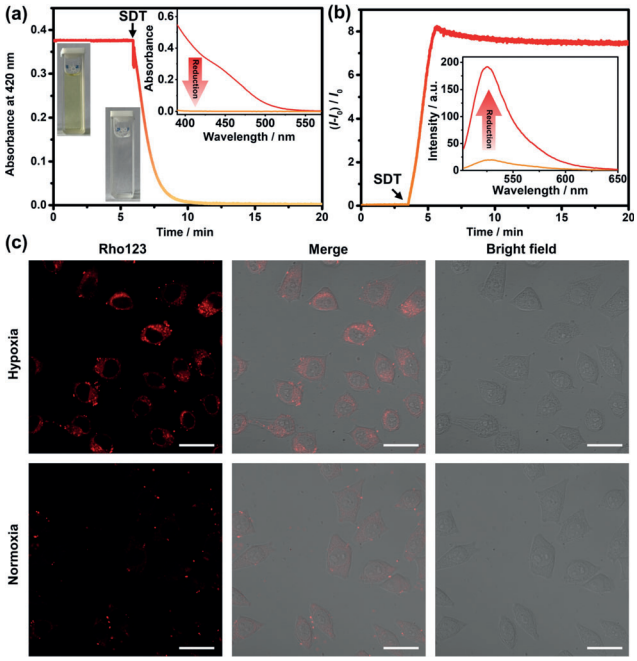

Figure 3. a) Absorbance at 420 nm of CAC4A (10 μM) as a function of time following addition of SDT (1.0 mM). Inset: Absorbance spectra of CAC4A (10 μM) before and after reduction by SDT (1.0 mM). b) Relative fluorescence intensity at 527 nm of CAC4A–Rho123 (30/10 μM) at different times after addition of SDT (1.0 mM). Inset: Fluorescence spectra of CAC4A–Rho123 (30/10 μM) before and after reducing by SDT (1.0 mM). Experimental conditions: PBS buffer, pH 7.4, 37°C. The slight decrease in fluorescence after the sharp increase may be caused by the partial reduction of Rho123 by the excess SDT. c) Confocal laser scanning microscopy images of A549 cells incubated with CAC4A–Rho123 under hypoxic (less than 0.1% O_2) or normoxic (20% O_2) conditions for 8 h. The Rho123 emission was obtained using excitation at 532 nm. Scale bar: 50 μm.

disappearance of the azo absorption indicates a complete reduction reaction i.e. all four azo groups of CAC4A were reduced (Figure 3a). The reducing kinetics were quantified by monitoring the absorbance at 420 nm in real time. The attenuation curve of the intensity was well fitted in a quasi-first-order reaction decay model (Adj. $R^2 > 0.993$), giving the rate constant of 0.905 min^{-1} (Supporting Information, Figure S9). The half-life was calculated as 46 s, which is at the same level of similar compounds containing a single azo group.[29] The reduction product of CAC4A was further examined by using mass spectrometry analysis. The mass spectrum of CAC4A shows peaks at 509 and 1017, corresponding to $[M+2H]^{2+}$ and $[M+H]^{+}$, respectively (Supporting Information, Figure S10a). Aminocalix[4]arene was found

after incubation with SDT, as shown by the appearance of peaks at 243, 485, and 969, corresponding to $[M+2H]^{2+}$, $[M+H]^{+}$, and $[2M+H]^{+}$, respectively (Supporting Information, Figure S10b). It indicates that all four azo groups of CAC4A were completely cleaved, in accordance with the UV/Vis results. Besides SDT, CAC4A could also be effectively and specifically reduced by reduced nicotinamide adenine dinucleotide phosphate (NADPH) in the presence of DT-diaphorase, a reductase that is upregulated in many cancers[30] and activated under hypoxic (Supporting Information, Figure S11) but not normoxic conditions (Supporting Information, Figure S12).

As expected, the fluorescence intensity of Rho123 was gradually restored in a time-dependent manner and reached saturation in two minutes with a marked eight-fold increase after adding SDT to the CAC4A–Rho123 complex (Figure 3b). Such a pronounced fluorescence increase demonstrates the feasibility of our host–guest approach in hypoxia imaging. The working principle is based on the differential binding between CAC4A and aminocalix[4]arene. CAC4A shows strong binding to Rho123 ($K_a = (1.4 \pm 0.1) \times 10^7\,M^{-1}$), while aminocalix[4]arene, as the reduction product, shows merely weak binding ($K_a = (5.4 \pm 0.8) \times 10^3\,M^{-1}$; Supporting Information, Figure S13) to Rho123. The K_a decrease of over three orders of magnitude results in the release of Rho123 and the corresponding fluorescence recovery after reducing CAC4A. To test the specificity of the hypoxia response, the fluorescence recovery was investigated by replacing SDT with other cellular reductants (cysteine, glutathione, reduced nicotinamide adenine dinucleotide, NADPH, and homocysteine) under both hypoxic and normoxic conditions (Supporting Information, Figure S14). No fluorescence enhancement was observed, indicating that the CAC4A–Rho123 complex is specifically responsive to hypoxia. Moreover, the acid tolerance of the reporter pair was investigated. At pH 5.0, CAC4A also binds strongly to Rho123 ($K_a = (1.5 \pm 0.4) \times 10^7\,M^{-1}$; Supporting Information, Figure S15). The comparable affinities between pH 7.4 and 5.0 eliminate the possibility of the undesired release of Rho123 triggered by acidic environments, which is meaningful for the following cell experiments when taking acidic conditions in the endosome/lysosome (about pH 5.0) into account.

With the aforementioned results in hand, the application of the CAC4A–Rho123 reporter pair in imaging hypoxia was explored. As a proof-of-concept, the utilization of CAC4A–Rho123 in hypoxia-selective imaging in living cells was investigated. A549 cancer cells were incubated with CAC4A–Rho123 in both normoxic and hypoxic conditions. As shown in Figure 3c, incubation of A549 cells with CAC4A–Rho123 under normoxia shows very low fluorescence signal. In contrast, when the cells were cultured under hypoxia, much brighter fluorescence was observed within the cells. These results prove that the CAC4A–Rho123 reporter pair was able to detect hypoxia in living cells.

Cellular probes for practical applications should minimally perturb living systems at the concentrations used. The cytotoxicity of CAC4A was evaluated by 3-(4,5-dimethylthiazol-2-yl)-2,5-diphenyltetrazolium bromide (MTT) assays[31] with various concentrations of CAC4A from 10 to 50 μM, under normoxic and hypoxic conditions (Supporting Information, Figure S16) for 24 h. Generally, even when loaded with a relatively high concentration of 50 μM, A549 cells exhibited a survival rate greater than 90% after incubation for 24 h under both normoxic and hypoxic conditions. These results suggest that under our experimental conditions (30 μM for 8 h incubation), CAC4A exhibited negligible cytotoxic effect against cells.

In conclusion, we demonstrate a new noncovalent strategy for imaging hypoxia based on the concept of supramolecular chemistry, which was validated in living cells. Compared with widely used covalent strategies, the present noncovalent strategy based on host–guest chemistry exhibits several intrinsic advantages: 1) the use of commercial probes without time- and cost-consuming synthesis; 2) releasing probes with high fidelity under hypoxia; 3) easy adaptability to other probes (and even treating agents) for constructing a universal platform. Such a noncovalent strategy is easily amenable to other azo-containing macrocycles for not only hypoxia-responsive imaging but also drug delivery. Noticeably, over 1200 azo-containing macrocycles have been reported up to now;[32] however, no hypoxia-responsive application has ever been demonstrated. This work not only paves a new way to imaging hypoxia but also explores new biomedical applications of azo macrocycles.

Acknowledgements

This work was supported by NSFC (51873090 and 21672112), the Fundamental Research Funds for the Central Universities and the Program of Tianjin Young Talents, which are gratefully acknowledged. The authors also thank Debin Zheng at College of Life Sciences, Nankai University for the mass spectrometry experiments.

Conflict of interest

The authors declare no conflict of interest.

Keywords: azo compound · calixarene · host–guest complex · hypoxia imaging · supramolecular chemistry

[1] a) J. M. Brown, W. R. Wilson, *Nat. Rev. Cancer* **2004**, *4*, 437–447; b) R. A. Gatenby, R. J. Gillies, *Nat. Rev. Cancer* **2008**, *8*, 56–61.
[2] Q. Chang, I. Jurisica, T. Do, D. W. Hedley, *Cancer Res.* **2011**, *71*, 3110–3120.
[3] B. A. Teicher, *Cancer Metastasis Rev.* **1994**, *13*, 139–168.
[4] Z. Huang, H. Xu, A. D. Meyers, A. I. Musani, L. Wang, R. Tagg, A. B. Barqawi, Y. K. Chen, *Technol. Cancer Res. Treat.* **2008**, *7*, 309–320.
[5] a) L. Schito, G. L. Semenza, *Trends Cancer* **2016**, *2*, 758–770; b) P. Vaupel, *Oncologist* **2008**, *13*, 21–26.
[6] a) A. M. Jubb, F. M. Buffa, A. L. Harris, *J. Cell. Mol. Med.* **2010**, *14*, 18–29; b) H. Minn, T. Gronroos, G. Komar, O. Eskola, K. Lehtio, J. Tuomela, M. Seppanen, O. Solin, *Curr. Pharm. Des.*

2008, *14*, 2932 – 2942; c) J. G. Rajendran, K. R. Hendrickson, A. M. Spence, M. Muzi, K. A. Krohn, D. A. Mankoff, *Eur. J. Nucl. Med. Mol. Imaging* **2006**, *33*, 44 – 53; d) H. Shi, X. Ma, Q. Zhao, B. Liu, Q. Qu, Z. An, Y. Zhao, W. Huang, *Adv. Funct. Mater.* **2014**, *24*, 4823 – 4830; e) Y. Zeng, Y. Liu, J. Shang, J. Ma, R. Wang, L. Deng, Y. Guo, F. Zhong, M. Bai, S. Zhang, D. Wu, *Plos One* **2015**, *10*, e0121293.

[7] S. Kizaka-Kondoh, M. Inoue, H. Harada, M. Hiraoka, *Cancer Sci.* **2003**, *94*, 1021 – 1028.

[8] a) K. Mikami, M. Naito, A. Tomida, M. Yamada, T. Sirakusa, T. Tsuruo, *Cancer Res.* **1996**, *56*, 2823 – 2826; b) Y. Shen, Q. Zhang, X. Qian, Y. Yang, *Anal. Chem.* **2015**, *87*, 1274 – 1280.

[9] a) A. Sharma, J. F. Arambula, S. Koo, R. Kumar, H. Singh, J. L. Sessler, J. S. Kim, *Chem. Soc. Rev.* **2019**, https://doi.org/10.1039/C8CS00304A; b) X. Li, N. Kwon, T. Guo, Z. Liu, J. Yoon, *Angew. Chem. Int. Ed.* **2018**, *57*, 11522 – 11531; *Angew. Chem.* **2018**, *130*, 11694 – 11704.

[10] a) J. Zhou, W. Shi, L.-H. Li, Q.-Y. Gong, X.-F. Wu, X.-H. Li, H.-M. Ma, *Chem. Asian J.* **2016**, *11*, 2719 – 2724; b) J. Zhang, H.-W. Liu, X.-X. Hu, J. Li, L.-H. Liang, X.-B. Zhang, W. Tan, *Anal. Chem.* **2015**, *87*, 11832 – 11839; c) Q.-Q. Wan, X.-H. Gao, X.-Y. He, S.-M. Chen, Y.-C. Song, Q.-Y. Gong, X.-H. Li, H.-M. Ma, *Chem. Asian J.* **2014**, *9*, 2058 – 2062; d) T. Guo, L. Cui, J. Shen, W. Zhu, Y. Xu, X. Qian, *Chem. Commun.* **2013**, *49*, 10820 – 10822; e) L. Cui, Y. Zhong, W. Zhu, Y. Xu, Q. Du, X. Wang, X. Qian, Y. Xiao, *Org. Lett.* **2011**, *13*, 928 – 931; f) H. S. Kim, A. Sharma, W. X. Ren, J. Han, J. S. Kim, *Biomaterials* **2018**, *185*, 63 – 72.

[11] a) K. Kiyose, K. Hanaoka, D. Oushiki, T. Nakamura, M. Kajimura, M. Suematsu, H. Nishimatsu, T. Yamane, T. Terai, Y. Hirata, T. Nagano, *J. Am. Chem. Soc.* **2010**, *132*, 15846 – 15848; b) A. Chevalier, W. Piao, K. Hanaoka, T. Nagano, P.-Y. Renard, A. Romieu, *Methods Appl. Fluoresc.* **2015**, *3*, 044004; c) Q. Cai, T. Yu, W. Zhu, Y. Xu, X. Qian, *Chem. Commun.* **2015**, *51*, 14739 – 14741; d) L. Sun, G. Li, X. Chen, Y. Chen, C. Jin, L. Ji, H. Chao, *Sci. Rep.* **2015**, *5*, 14837; e) F. Perche, S. Biswas, T. Wang, L. Zhu, V. P. Torchilin, *Angew. Chem. Int. Ed.* **2014**, *53*, 3362 – 3366; *Angew. Chem.* **2014**, *126*, 3430 – 3434; f) A. Popat, B. P. Ross, J. Liu, S. Jambhrunkar, F. Kleitz, S. Z. Qiao, *Angew. Chem. Int. Ed.* **2012**, *51*, 12486 – 12489; *Angew. Chem.* **2012**, *124*, 12654 – 12657; g) P. Yuan, H. Zhang, L. Qian, X. Mao, S. Du, C. Yu, B. Peng, S. Q. Yao, *Angew. Chem. Int. Ed.* **2017**, *56*, 12481 – 12485; *Angew. Chem.* **2017**, *129*, 12655 – 12659.

[12] W. Piao, S. Tsuda, Y. Tanaka, S. Maeda, F. Liu, S. Takahashi, Y. Kushida, T. Komatsu, T. Ueno, T. Terai, T. Nakazawa, M. Uchiyama, K. Morokuma, T. Nagano, K. Hanaoka, *Angew. Chem. Int. Ed.* **2013**, *52*, 13028 – 13032; *Angew. Chem.* **2013**, *125*, 13266 – 13270.

[13] M. I. Uddin, S. M. Evans, J. R. Craft, L. J. Marnett, M. J. Uddin, A. Jayagopal, *ACS Med. Chem. Lett.* **2015**, *6*, 445 – 449.

[14] a) X. Ma, Y. Zhao, *Chem. Rev.* **2015**, *115*, 7794 – 7839; b) J. Gao, J. Li, W.-C. Geng, F.-Y. Chen, X. Duan, Z. Zheng, D. Ding, D.-S. Guo, *J. Am. Chem. Soc.* **2018**, *140*, 4945 – 4953.

[15] A. Norouzy, Z. Azizi, W. M. Nau, *Angew. Chem. Int. Ed.* **2015**, *54*, 792 – 795; *Angew. Chem.* **2015**, *127*, 804 – 808.

[16] a) V. Böhmer, *Angew. Chem. Int. Ed. Engl.* **1995**, *34*, 713 – 745; *Angew. Chem.* **1995**, *107*, 785 – 818; b) M. A. Beatty, J. Borges-Gonzalez, N. J. Sinclair, A. T. Pye, F. Hof, *J. Am. Chem. Soc.* **2018**, *140*, 3500 – 3504.

[17] Y. Morita, T. Agawa, E. Nomura, H. Taniguchi, *J. Org. Chem.* **1992**, *57*, 3658 – 3662.

[18] V. Reshetnikov, S. Daum, C. Janko, W. Karawacka, R. Tietze, C. Alexiou, S. Paryzhak, T. Dumych, R. Bilyy, P. Tripal, B. Schmid, R. Palmisano, A. Mokhir, *Angew. Chem. Int. Ed.* **2018**, *57*, 11943 – 11946; *Angew. Chem.* **2018**, *130*, 12119 – 12122.

[19] a) D.-S. Guo, H.-Q. Zhang, F. Ding, Y. Liu, *Org. Biomol. Chem.* **2012**, *10*, 1527 – 1536; b) Z. Zheng, W.-C. Geng, J. Gao, Y.-Y. Wang, H. Sun, D.-S. Guo, *Chem. Sci.* **2018**, *9*, 2087 – 2091.

[20] a) P. J. Stephens, F. J. Devlin, C. F. Chabalowski, M. J. Frisch, *J. Phys. Chem.* **1994**, *98*, 11623 – 11627; b) A. D. Becke, *J. Chem. Phys.* **1993**, *98*, 5648 – 5652; c) P. C. Hariharan, J. A. Pople, *Theor. Chim. Acta* **1973**, *28*, 213 – 222; d) W. J. Hehre, R. Ditchfield, J. A. Pople, *J. Chem. Phys.* **1972**, *56*, 2257 – 2261.

[21] J. S. Murray, P. Politzer, *WIREs Comput. Mol. Sci.* **2011**, *1*, 153 – 163.

[22] C. Lefebvre, G. Rubez, H. Khartabil, J. C. Boisson, J. Contreras-Garcia, E. Henon, *Phys. Chem. Chem. Phys.* **2017**, *19*, 17928 – 17936.

[23] A. Chevalier, C. Mercier, L. Saurel, S. Orenga, P. Y. Renard, A. Romieu, *Chem. Commun.* **2013**, *49*, 8815 – 8817.

[24] J. R. Lakowicz, *Principles of Fluorescence Spectroscopy*, Springer US, New York, **2006**.

[25] a) R. N. Dsouza, U. Pischel, W. M. Nau, *Chem. Rev.* **2011**, *111*, 7941 – 7980; b) D.-S. Guo, V. D. Uzunova, X. Su, Y. Liu, W. M. Nau, *Chem. Sci.* **2011**, *2*, 1722 – 1734.

[26] A. Weller, *Pure Appl. Chem.* **1968**, *16*, 115 – 123.

[27] A. P. de Silva, H. Q. N. Gunaratne, T. Gunnlaugsson, A. J. M. Huxley, C. P. McCoy, J. T. Rademacher, T. E. Rice, *Chem. Rev.* **1997**, *97*, 1515 – 1566.

[28] a) G. Leriche, G. Budin, L. Brino, A. Wagner, *Eur. J. Org. Chem.* **2010**, 4360 – 4364; b) Y. Y. Yang, M. Grammel, A. S. Raghavan, G. Charron, H. C. Hang, *Chem. Biol.* **2010**, *17*, 1212 – 1222.

[29] P. Verwilst, J. Han, J. Lee, S. Mun, H.-G. Kang, J. S. Kim, *Biomaterials* **2017**, *115*, 104 – 114.

[30] a) J. Rao, A. Khan, *J. Am. Chem. Soc.* **2013**, *135*, 14056 – 14059; b) J. Rao, C. Hottinger, A. Khan, *J. Am. Chem. Soc.* **2014**, *136*, 5872 – 5875; c) R. Li, M. A. Bianchet, P. Talalay, L. M. Amzel, *Proc. Natl. Acad. Sci. USA* **1995**, *92*, 8846 – 8850.

[31] T. Mosmann, *J. Immunol. Methods* **1983**, *65*, 55 – 63.

[32] W.-C. Geng, H. Sun, D.-S. Guo, *J. Inclusion Phenom. Macrocyclic Chem.* **2018**, *92*, 1 – 79.

Manuscript received: November 23, 2018
Revised manuscript received: January 8, 2019
Accepted manuscript online: January 10, 2019
Version of record online: ■■ ■■, ■■■■

Communications

Imaging Agents

W.-C. Geng, S. Jia, Z. Zheng, Z. Li, D. Ding, D.-S. Guo* _____ ■■■–■■■

A Noncovalent Fluorescence Turn-on Strategy for Hypoxia Imaging

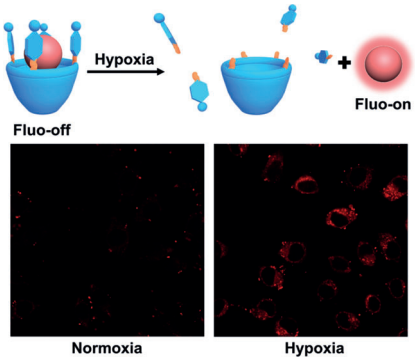

A supramolecular strategy for fluorescent hypoxia imaging is proposed based on the host–guest complexation of azomacrocycles with commercial dyes.